The Multigrid Image Transform

Paul M. de Zeeuw

CWI, P.O. Box 94079, 1090 GB Amsterdam, The Netherlands. E-mail:
Paul.de.Zeeuw@cwi.nl

Summary. A second order partial differential operator is applied to an image function. To this end we consider both the Laplacian and a more general elliptic operator. By using a multigrid operator known from the so-called approximation property, we derive a multiresolution decomposition of the image without blurring of edges at coarser levels. We investigate both a linear and a nonlinear variant and compare to some established methods.

Key words: Elliptic multigrid image transform, gradient pyramids, Laplace equation, Laplacian pyramids, Laplacian multigrid image transform, lifting scheme, multigrid methods, multiresolution, steerable pyramids, wavelets.

1 Introduction

In a more or less parallel development the idea of multiresolution has become an important instrument both in the field of signal processing and in the field of numerical methods for the solution of partial differential equations (PDEs). With respect to the latter we allude to the *multigrid* type of method which solves discretized elliptic, parabolic and hyperbolic PDEs as well as integral equations by accelerating a basic iterative solution process through adequate coarse grid corrections [5, 14]. A historical overview of the development including a list of pioneering papers is given by Wesseling [26].

Terzopoulos [23] was the first to apply multigrid for image analysis. More recently, the use of multigrid for image processing purposes has been proposed by Acton [1], Kimmel et al. [16], Shapira [20], Ke Chen et al. [9], Bruhn et al. [6] and others. However, its use is restricted to the efficient solution of partial differential equations (typically diffusion and Euler-Lagrange equations) which could also be achieved by other means.

De Zeeuw (this author) started to use multigrid operators as an intrinsic and indissoluble part of the so-called *multigrid image transform* [13]. In this

scheme, first a second order partial differential operator is applied to an image function followed by a pyramidal decomposition using typical multigrid operators. The case of isotropic homogeneous diffusion (Poisson) provides an example that leads to a linear multiresolution scheme. It can be applied successfully with respect to image fusion [13].

In the present paper we consider a general elliptic operator but we focus on the isotropic inhomogeneous diffusion operator, with coefficients in the fashion of Perona and Malik [18, 19]. It leads to a nonlinear multiresolution scheme. A future application of the new scheme might be in image fusion using a nonlinear multiresolution decomposition implying a multisource segmentation.

The paper is organized as follows. After a recapitulation on multigrid in Section 2 we discuss the multigrid image transform in Section 3. In particular we consider one that is associated with the Laplacian (leading to a linear multiresolution scheme) and one that is associated with a more general elliptic partial differential operator (leading to a nonlinear multiresolution scheme). We show results of the transforms in Section 4 and compare to other multiresolution schemes amongst which a nonlinear one by Heijmans and Goutsias [15]. We end up with concluding remarks.

2 Recapitulation on Multigrid

A prohibitive problem with the solution of large (non)linear systems of equations is that the number of arithmetic operations involved is more than linearly proportional to the number of unknowns. For example, the complexity of the direct solution of large sparse linear systems is still quadratic even when exploiting the structured sparsity. Also the fill-in demands more than proportional storage. Such systems arise after the discretization of PDEs on a spatial grid. For special PDEs, e.g. Poisson problems, considerable efficiency can yet be achieved, for an overview see e.g. Botta et al. [4].

Multigrid is a numerical class of methods which tackles the complexity problem head-on by representing and solving a problem and its derivations on a sequence of increasingly coarser (finer) grids. Nowadays extensive literature is available on multigrid. We merely point to Brandt [5], Hackbusch [14], Wesseling [26] and (more recent) to Trottenberg et al. [24] and Shapira [20].

Here we recapitulate particular items that we need for the multigrid transform to be discussed from an article by De Zeeuw (this author) on a robust multigrid algorithm for the numerical solution of (scalar) diffusion and convection-diffusion problems [10]. The algorithm has been implemented and exists by the name of MGD9V. Tests demonstrate its (optimal) complexity for a wide range of problems known to be difficult to solve. It employs a set of rectangular and increasingly coarser grids (vertex-centered):

$$\Omega_n \supset \Omega_{n-1} \supset \ldots \Omega_k \supset \ldots \supset \Omega_0.$$

The grids are described as follows:

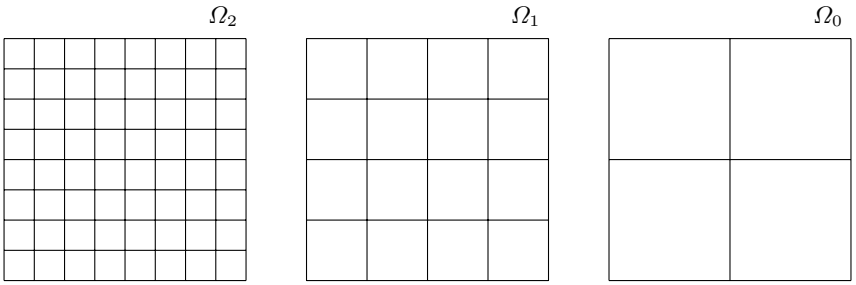

Fig. 1. Example sequence of increasingly coarsened grids used in multigrid (vertex-centered)

$$\Omega_k \equiv \{(x_i, y_i) \mid x_i = o_1 + (i-1)h_k, y_i = o_2 + (j-1)h_k\} \tag{1}$$

where (o_1, o_2) is the origin and $h_{k-1} = 2h_k$. See Figure 1 for an example. $S(\Omega_k)$ denotes the linear space of real-valued functions on Ω_k

$$S(\Omega_k) = \{g_k \mid g_k : \Omega_k \to \mathbb{R}\},$$

where $g_k \in S(\Omega_k)$ is called a *grid-function*. The algorithm is intended for the solution of linear systems resulting from the 9-point discretization of the following general linear second-order elliptic partial differential equation in two dimensions:

$$Lu \equiv -\nabla \cdot (D(x)\nabla u(x)) + b(x) \cdot \nabla u(x) + c(x)u(x) = f(x) \tag{2}$$

on a bounded domain $\Omega \subset \mathbb{R}^2$ with suitable boundary conditions. $D(x)$ is a positive definite 2×2 matrix function and $c(x) \geq 0$. It is assumed that the discretization of (2) is performed by a finite element or finite volume technique, leading to

$$L_n \overline{u}_n = f_n \tag{3}$$

where

$$L_n \quad : \quad S(\Omega_n) \to S(\Omega_n) \tag{4}$$

is the discretization of L and $f_n \in S(\Omega_n)$ is the discretization of f. Grid-function $\overline{u}_n$ is the solution that is looked for. The solution algorithm uses *sawtooth multigrid cycles*, that is, a smoother is applied after the coarse grid correction (CGC). Let u_n be an approximation of $\overline{u}_n$. The CGC at level k reads:

$$r_k = f_k - L_k u_k; \tag{5}$$

$$r_{k-1} = R_{k-1} r_k; \tag{6}$$

$$\text{solve (approximately)} \quad L_{k-1} e_{k-1} = r_{k-1}; \tag{7}$$

$$\tilde{u}_k = u_k + P_k e_{k-1}. \tag{8}$$

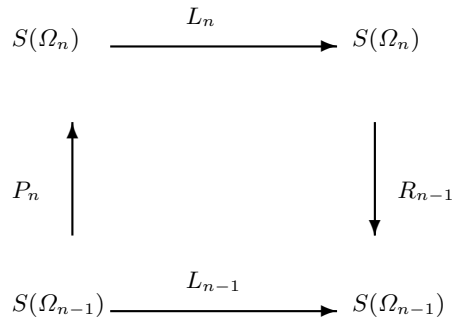

Fig. 2. Diagram of Galerkin approximation

It is immediately followed by:

$$\tilde{\tilde{u}}_k = \text{SMOOTH}(f_k, L_k, \tilde{u}_k). \tag{9}$$

In MGD9V the particular choice for SMOOTH() is *Incomplete Line LU factorization* (for a description see [11] and the references mentioned there). The grid transfer operators are defined as follows.

$$R_{k-1} \quad : \quad S(\Omega_k) \to S(\Omega_{k-1}), \quad k = n, \ldots, 1 \tag{10}$$

is the restriction operator that transfers the residual from the grid Ω_k onto the coarser grid Ω_{k-1}, and

$$P_k \quad : \quad S(\Omega_{k-1}) \to S(\Omega_k), \quad k = 1, \ldots, n \tag{11}$$

is the prolongation operator that interpolates and transfers a correction for the solution from the coarser towards the finer grid. The operator L_{k-1} is defined by the sequence of operations

$$L_{k-1} \equiv R_{k-1} L_k P_k, \quad k = n, \ldots, 1 \tag{12}$$

known as the *Galerkin coarse grid approximation*. One cycle of sawtooth multigrid is defined by application of (5)–(9) for $k = n$. A recursion enters at stage (7). The system of equations at this stage is approximated by applying again the above cycle, but now at level $k - 1$. (At level 0 mere smoothing is performed).

The diagram of Figure 2 illustrates the coherence of the afore mentioned operators. We choose the restriction to be the transpose of the prolongation

$$R_{k-1} = P_k^T, \quad k = n, \ldots, 1. \tag{13}$$

Hence, once P_k has been chosen, R_{k-1} and L_{k-1} follow automatically. One actually computes the coarse grid matrix of L_{k-1}. Note that by (13) the

possible (anti)symmetry of L_k is maintained on the coarser grid. Further, it has been proved [10] that when L_k is a conservative discretization of L and P_k interpolates a constant function exactly, then the Galerkin approximation L_{k-1} is conservative as well. In the case of e.g. the Poisson equation and discretization by bilinear finite elements, bilinear interpolation is the natural choice for P_k. This case is discussed in Section 3.2. In the case of discontinuous diffusion coefficients a far more sophisticated choice is required [10]. This case is discussed in Section 3.3.

Adiabatic Boundary Conditions

At the boundaries of Ω one often assumes vanishing Neumann boundary conditions. At Ω_n we discretize them in a conservative fashion, e.g. by using bilinear finite elements. The following statements can all be derived from [10]. The boundary conditions inherited by L_k, $0 \leq k < n$, remain vanishing Neumann ones. All L_k, $0 \leq k \leq n$ have a singular matrix and therefore the L_k^{-1} do not exist. However, systems of type $L_k u_k = g_k$ can still be solved, provided that g_k is in the range of L_k. A sufficient and necessary condition for the latter is proved to be that the sum of elements of g_k vanishes. The said discretization warrants this condition for $k = n$. Further, it is proved that $R_{k-1} g_k$ inherits the condition. It follows that the multigrid algorithm in [10] is able to solve the described systems iteratively, even though the matrix L_n is singular. The solution u_k is unique up to a constant (grid-function).

3 The Multigrid Image Transform

3.1 Introduction

So far, we have recapitulated how a multigrid method solves large linear systems of equations arising from discretized PDEs in a very efficient manner based on a recursive procedure. However, the current section is not about multigrid solution methods, but about image *transforms* involving multigrid operators. The exploits of Section 2 provide some necessary tools for the transforms to be discussed. Another tool that we need is the multigrid approximation operator

$$E_k \quad : \quad S(\Omega_k) \rightarrow S(\Omega_k), \quad k = 1, \ldots, n \tag{14}$$

which is defined as:

$$E_k \equiv L_k^{-1} - P_k L_{k-1}^{-1} R_{k-1}, \quad k = 1, \ldots, n. \tag{15}$$

It is associated with the so-called *approximation property*. Under a certain regularity of the boundary value problem (2), a discretization (3) by (bilinear) finite elements, and P_k is bilinear interpolation, it can be shown that (see Hackbusch [14, §6.3]):

$$\|E_k\|_2 \quad \leq \quad Ch_k^2 \tag{16}$$

where h_k is the mesh-size of Ω_k and $\|\cdot\|_2$ is the Euclidean norm on $S(\Omega_k)$. This operator plays an important role in convergence proofs in multigrid theory. In [13] it has been proposed to let E_k serve a practical purpose as well. There it is introduced as a high-pass filter in a multiresolution scheme: the *multigrid image transform*[13]. The transform reads as follows. Let u_n be an image, defined as a grid-function on $S(\Omega_n)$. Then compute grid-function $f_n = L_n u_n$, for the definition of L_n see (2) and (3). Note that this is contrary to finding a solution u_n for given f_n, which was the problem stated in Section 2. An important example for L_n is the discretized Laplacian operator, this is discussed in Section 3.2. Let

$$f_k \equiv R_k f_{k+1}, \quad k = n-1, \ldots, 0 \tag{17}$$

then we define the *multigrid image transform* or *multigrid image decomposition* as follows

$$\begin{cases} a_0 & = & L_0^{-1} f_0, \\ d_k & = & E_k f_k, \quad k = 1, \ldots, n. \end{cases} \tag{18}$$

The a_k are called *approximations* and the d_k are called *details*. The reconstruction counterpart reads:

$$a_k = P_k a_{k-1} + d_k, \quad k = 1, \ldots, n. \tag{19}$$

Regarding (3), (10)–(12), (15), (17)–(19) it follows that

$$L_k a_k = f_k, \quad k = 0, \ldots, n.$$

which implies that the reconstruction (19) with respect to the decomposition (18) is a perfect one. The proof can be found in a previous paper [13].

As with other multiresolution methods, manipulations of the detail coefficients d_k may allow for a better tackling of image processing problems.

Adiabatic Boundary Conditions Revisited

Under these boundary conditions E_k is meaningful, even though it is not defined in the strict sense. It can be proved that if g_k is in the range of L_k then $R_{k-1} g_k$ is in the range of L_{k-1} and therefore $E_k g_k$ can still be applied. Again, the result is unique up to a constant (grid-function).

3.2 The Laplacian Multigrid Image Transform

Laplacian

Firstly, we consider the case of both isotropic and homogeneous diffusion which boils down to the use of the Laplacian operator $-\Delta$. Let L_n be the discretization on the grid Ω_n (uniform and rectangular). If discretized by

means of bilinear finite elements (or volumes) it gives rise to the following 3×3 stencil (or mask) for meshsize 1:

$$L_n \sim \frac{1}{3}\begin{bmatrix} -1 & -1 & -1 \\ -1 & +8 & -1 \\ -1 & -1 & -1 \end{bmatrix}. \tag{20}$$

Bilinear Prolongation

Under the assumption of (13), the prolongation must satisfy an accuracy condition, in order to obtain mesh-size independent rate of multigrid convergence. Such an accuracy condition is increasingly stringent for higher orders of the PDE, for more details see [5, 14, 26]. Here, bilinear interpolation satisfies the accuracy condition for the second order PDE. This interpolation amounts to taking an equal average of solution-values at neighbouring coarse-grid points, see Figure 3 for an illustration. At the grid-points of the fine grid that coincide

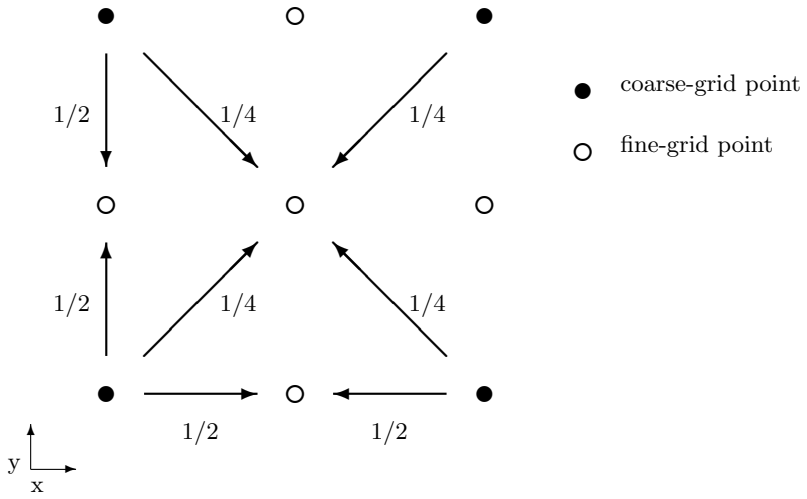

Fig. 3. Bilinear prolongation.

with the coarse grid we take identical values. The bilinear prolongation can also be denoted by the stencil

$$P_k \sim \begin{bmatrix} \frac{1}{4} & \frac{1}{2} & \frac{1}{4} \\ \frac{1}{2} & 1 & \frac{1}{2} \\ \frac{1}{4} & \frac{1}{2} & \frac{1}{4} \end{bmatrix}. \tag{21}$$

This stencil shows the non-zero values of the fine-grid function generated by the prolongation of a coarse-grid function which equals 1 at one point and 0 elsewhere. Because of (13), the same stencil also represents the chosen restriction operator.

Ease of Implementation

With the prolongation and restriction thus chosen the Laplacian stencil (20) is invariant on the coarser grids. That is, all L_k produced by (12) turn out to be represented by the same stencil on the subsequently coarser grids $S(\Omega_k)$, $0 \leq k < n$. We assume adiabatic boundary conditions which are also retained. The proof can be derived from [10].

Through this foreknowledge the multigrid method can be simplified greatly with respect to its implementation. It is not necessary to perform (12) explicitly as we already know the outcome both in the interior and at the boundaries. Another simplification lies in the choice of the basic iterative method (also known as smoother or relaxation method). With the above Laplacian stencil one can resort to simple and vectorizable smoothers like e.g. damped Jacobi. Moreover, the method becomes economical with computer memory as storage of matrices and their decompositions is not required.

3.3 The Elliptic Multigrid Image Transform

Matrix-dependent Prolongations and Restrictions

We recall the elliptic operator (2) defined in Section 2. We add that the positive definite tensor D is allowed to be discontinuous across an interface Γ in the interior of Ω. Obviously, definitions of coefficients in the fashion of Perona and Malik allow for this to happen. Let L_n be the discretization on Ω_n (uniform and rectangular grid) by means of bilinear finite elements (or volumes). When D is strongly discontinuous, multigrid with bilinear prolongation becomes excruciatingly slow: the number of iterative cycles necessary to obtain a fixed reduction of r_n becomes prohibitively large. The explanation is as follows. Let $n = n(x)$ be the normal at Γ. Then, as has been argued by Alcouffe et al. [2], continuity of $n \cdot (D\nabla u)$ instead of continuity of ∇u should be the underlying assumption for interpolation. This leads to jump conditions that need to be satisfied across interfaces. Only in the (special) case that the diffusion coefficient D is continuous, it follows that ∇u is continuous as well and the use of bilinear interpolation is justified. For an illustrative one-dimension example on interface problems see Hackbusch [14, §10.3.1]. The right assumption that $n \cdot (D\nabla u)$ is continuous leads to the remedy of operator-dependent prolongations (and restrictions). Figure 4 provides an *in situ* illustration of a biased prolongation, satisfying a jump condition for the case that the diffusion coefficient is negligible in the shaded region. One notes the obvious differences with Figure 3.

In [10] a matrix-dependent prolongation operator has been proposed, able to handle both the case of (dominant) advection and interface problems at the same time. Here we give a brief outline of the operator. At each level k the (black box) multigrid algorithm derives the necessary information on the operator coefficients from the matrix L_k (this explains the adjective "matrix-dependent"). The grid Ω_k is split into four disjoint sub-grids as follows:

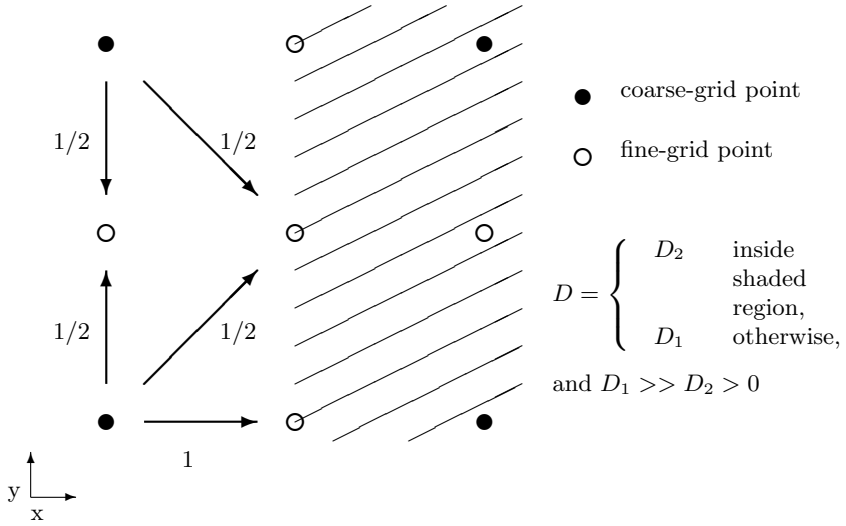

Fig. 4. Example of biased prolongation.

$\Omega_{k,(0,0)} \equiv \Omega_{k-1}$,
$\Omega_{k,(1,0)} \equiv \{(x + h_k, y) \in \Omega_k \mid (x, y) \in \Omega_{k-1}\}$,
$\Omega_{k,(0,1)} \equiv \{(x, y + h_k) \in \Omega_k \mid (x, y) \in \Omega_{k-1}\}$,
$\Omega_{k,(1,1)} \equiv \{(x + h_k, y + h_k) \in \Omega_k \mid (x, y) \in \Omega_{k-1}\}$,

where h_k is the mesh-size of grid Ω_k. We proceed as follows.

1. At the fine-grid points in $\Omega_{k,(0,0)}$, we simply adopt the values on Ω_{k-1}.
2. Let $\xi \in \Omega_{k,(1,0)}$ be a point where we have to interpolate a coarse grid correction. It is by definition located on a horizontal grid-line between two neighbouring points at Ω_{k-1}. Locally, we decompose the matrix L_k in its symmetric and antisymmetric part. The symmetric part is presumed to correspond with diffusion and the zeroth order term, the antisymmetric part with convection. We reconstruct the various operator coefficients at ξ and apply essentially one-dimensional interpolation. The interpolation coefficients are stored.
3. Let $\xi \in \Omega_{k,(0,1)}$ be a point where we have to interpolate a coarse grid correction. We interpolate as above, but now on a vertical grid-line of Ω_{k-1}.
4. At the fine-grid points in $\Omega_{k,(1,1)}$, we solve the homogeneous equation (with respect to L_k) to obtain the correction.
5. Now that P_k has been defined (and therefore R_{k-1} as well) we compute L_{k-1} according to (12) at the next coarser grid and we repeat the whole process above for level $k - 1$ ($k > 0$).

Definition

Summarizing, the *elliptic multigrid image transform* is defined by (17)–(18), through the elliptic operator L and its discretization L_n (see (2) and (3)), through the matrix-dependent P_k and (12)–(13). The Laplacian multigrid image transform of Section 3.2 is a particular example of this transform.

Implementation

The implementation of the actual computation of L_{k-1} according to (12) with the above matrix-dependent P_k is far from trivial. The implementation of a highly robust smoother like e.g. incomplete line LU factorization is also not a trivial matter, but it is what the multigrid method wants due to the discontinuous diffusion coefficients. For these reasons, the general elliptic multigrid image transform is more intricate than the Laplacian one. Nevertheless, the necessary work is of low and linear complexity. (The stencils L_k do not grow on the coarser grids but remain 3×3 just like L_n.)

4 Comparative Results

Perona and Malik Type Diffusivity

For experiments with the elliptic multigrid transforms we limit ourselves to the case of no convection and no zeroth order term. With respect to the diffusivity we consider diffusion which is again isotropic but inhomogeneous. It boils down to the use of the operator $-\nabla \cdot (D\nabla u)$ where D is scalar-valued, not a tensor (several possibilities exist for D as tensor as pointed out by Weickert [25]). Perona and Malik [18, 19] have reasoned that intra-region smoothing should occur preferentially over inter-region smoothing. The diffusion is chosen locally as a function of the magnitude of the gradient of the image function

$$D(x) = g(|\nabla u(x)|^2). \tag{22}$$

With respect to the function g we opt here for the following:

$$g(s) = \frac{1}{\sqrt{(1+s)}} \tag{23}$$

see Aubert et al. [3, §3.3.1] for a full motivation. In the context of the Perona-Malik model this gives better smoothing in the tangential direction than in the normal direction.

Discretized, this diffusivity expresses the coupling that exists between points in the image. By means of (12) this coupling is transferred to coarser grids. The matrix-dependent grid transfer operators secure that weak (strong) couplings remain weak (strong). Therefore, as with time integration, the diffusivity helps to preserve edges (but now on coarsened grids).

Experiments

We apply both the Laplacian and the elliptic multigrid transform with the above diffusion operator, both with adiabatic boundary conditions, to the grayscale image at the top of Figure 5. We compare with the results of well-known linear multiresolution schemes as wavelets [17] (see Figure 5) and Laplacian pyramids [7], gradient pyramids [8] and steerable pyramids [21] (see Figure 6).

Further, in Figure 7, we compare with the results of what we refer to as the "maxmin-lifting scheme". This scheme is a nonlinear version of the lifting scheme [22] involving quincunx grids. It is defined by intertwined use of the nonlinear max- and min-lifting schemes by Heijmans and Goutsias [15]. The max-lifting scheme has the property that it preserves local maxima over several scales. The min-lifting scheme has a similar property with respect to local minima. An implementation of the maxmin-lifting scheme can be found through [12]. Clearly, Figure 7 depicts the least blurring of edges on subsequently coarsened grids.

Efficiency

Table 1 shows CPU times consumed on a 2.16 GHz processor by a few selected multiresolution schemes (decomposition plus reconstruction) on grids with different dimensions. The costs of the schemes appear to be within the same

Table 1. CPU seconds consumed by multiresolution schemes

Grid	Daubechies 4	maxmin-lifting	elliptic MG
256×256	0.43	0.45	0.30
512×512	0.74	0.94	0.79
1024×1024	2.40	3.82	3.08

range. Moreover, the measurements accord with the claimed computational complexities.

5 Concluding Remarks

New multiresolution schemes have been investigated, based on an image transform by a discretized elliptic partial differential operator and use of a multigrid operator, leading to pyramidal representations. Depending on the differential operator, the scheme is linear or nonlinear. The linear scheme (Laplacian multigrid image transform) is easy to implement, rapidly converging and economical with storage. An example of the nonlinear scheme (elliptic multigrid

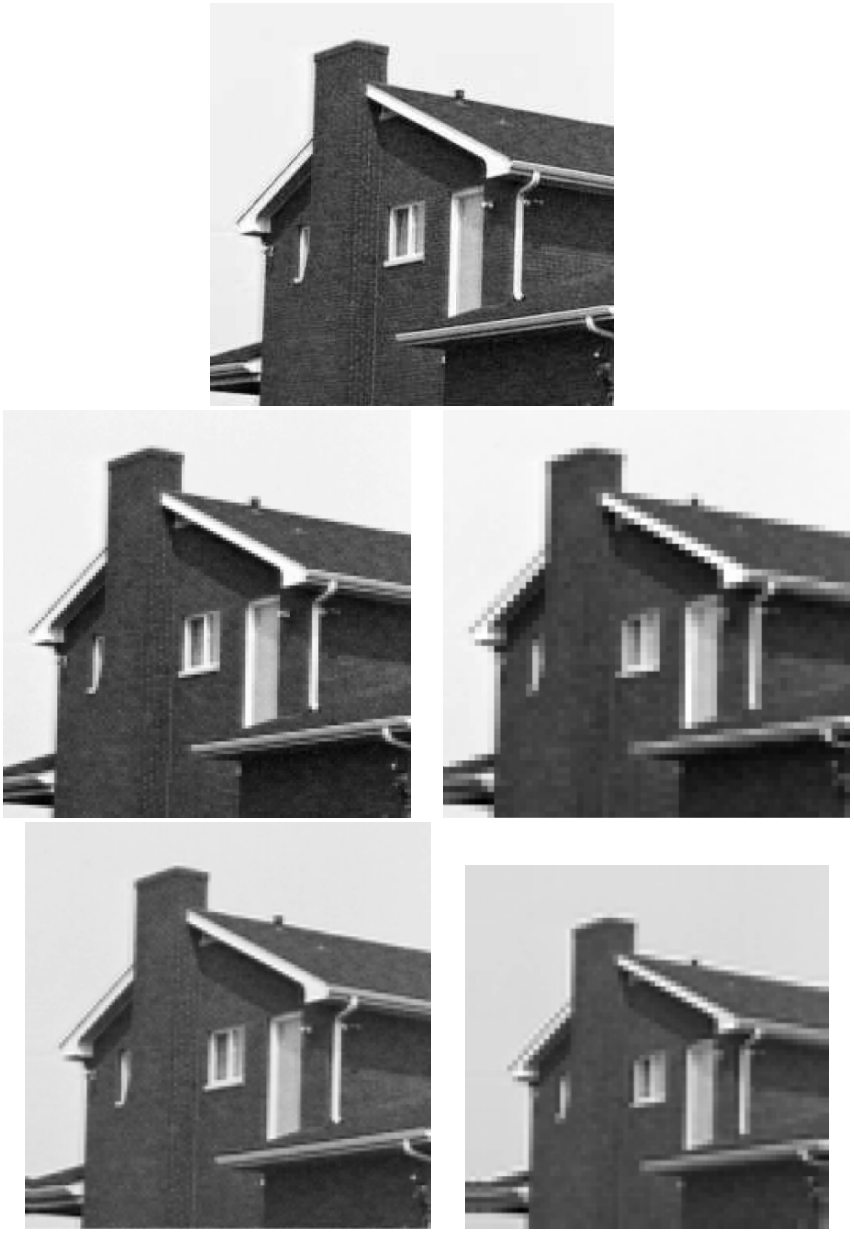

Fig. 5. Top: original image. Middle and bottom row show approximations on subsequently coarsened grids (from left to right). Middle row: Haar wavelet decomposition. Bottom row: wavelet decomposition by Daubechies 4.

Fig. 6. Approximations on subsequently coarsened grids (from left to right). Top row: Laplacian pyramid. Middle row: gradient pyramid. Bottom row: steerable pyramid (6 bands).

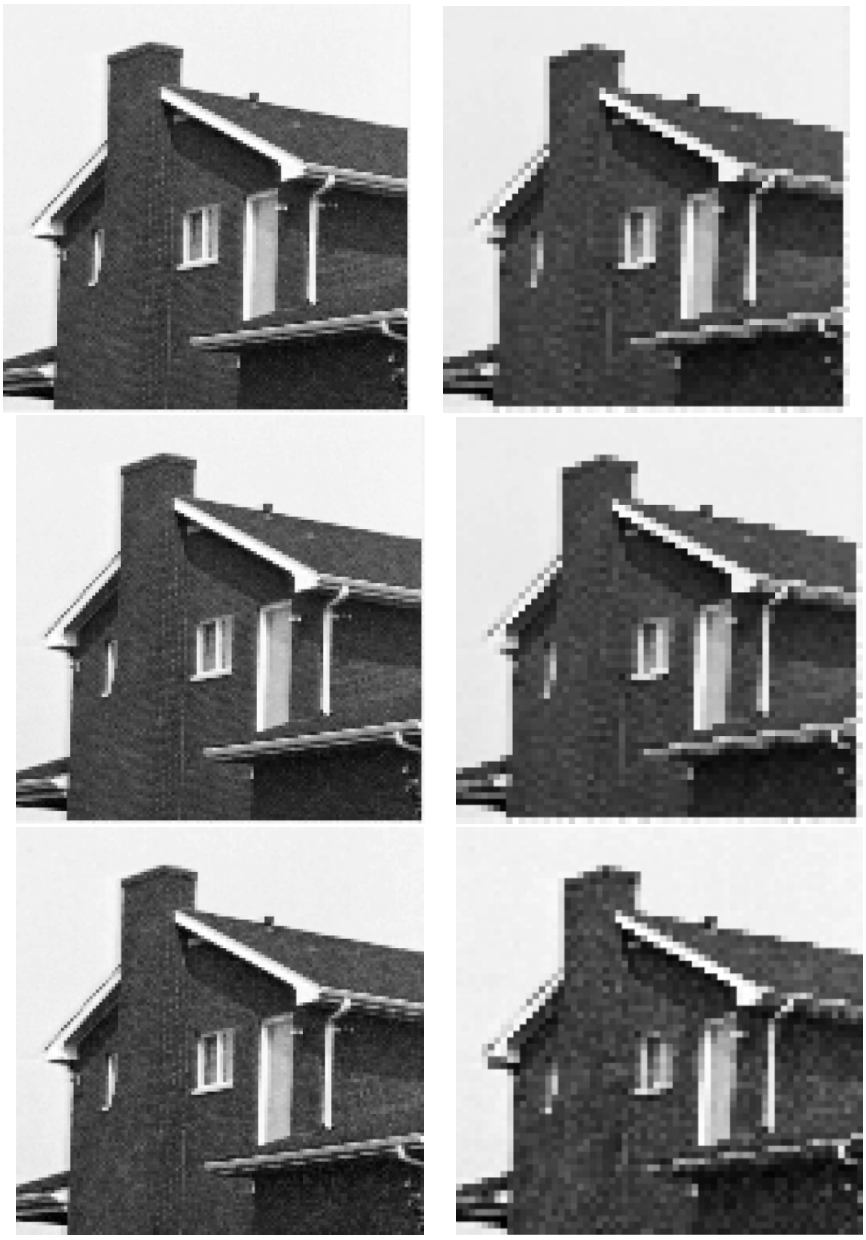

Fig. 7. Approximations on subsequently coarsened grids (from left to right). Top row: Laplacian multigrid image transform. Middle row: elliptic multigrid image transform. Bottom row: maxmin-lifting scheme.

image transform) based on Perona and Malik type diffusivity has been developed. Though more intricate than the linear scheme, the complexity remains low and linear. A comparison with several well-known and established linear multiresolution schemes has been made, but also with a nonlinear lifting scheme. The latter scheme and both multigrid image transforms appear to be in the same league with respect to preservation of edges at coarser grids. The elliptic multigrid image transform appears to have a slight edge over the nonlinear lifting scheme.

So far, we have considered mere scalar diffusion. A diffusion tensor leading to anisotropic (tensor) diffusion filters [25] with special spatial regularization properties could be a topic for future research. Another future topic could be image fusion, as the elliptic multigrid image transform appears to relate to segmentation.

References

1. S. T. Acton. Multigrid anisotropic diffusion. *IEEE Trans. Image Process.*, 7(3):280–291, 1998.
2. R. E. Alcouffe, A. Brandt, J. E. Dendy, and J. W. Painter. The multi–grid method for the diffusion equation with strongly discontinuous coefficients. *SIAM J. Sci. Statist. Comput.*, 2:430–454, 1981.
3. G. Aubert and P. Kornprobst. *Mathematical Problems in Image Processing, Partial Differential Equations and the Calculus of Variations*, volume 147 of *Applied Mathematical Sciences*. Springer Verlag, New York, 2002.
4. E. F. F. Botta, K. Dekker, Y. Notay, A. van der Ploeg, C. Vuik, F. W. Wubs, and P. M. de Zeeuw. How fast the Laplace equation was solved in 1995. *J. Applied Numerical Mathematics*, 24:439–455, 1997.
5. A. Brandt. Multi–level adaptive techniques (mlat) for partial differential equations: ideas and software. In J. R. Rice, editor, *Mathematical Software III*, pages 277–318. Academic Press, New York, 1977.
6. A. Bruhn, J. Weickert, T. Kohlberger, and C. Schnörr. Discontinuity-preserving computation of variational optic flow in real-time. In R. Kimmel, N. Sochen, and J. Weickert, editors, *Scale Space and PDE Methods in Computer Vision*, volume 3459 of *Lecture Notes in Computer Science*, pages 279–290. Springer-Verlag, Berlin Heidelberg, 2005.
7. P. J. Burt and E. H. Adelson. The laplacian pyramid as a compact image code. *IEEE Transactions on Communications*, 31(4):532–540, 1983.
8. P. J. Burt and R. J. Kolczynski. Enhanced image capture through fusion. In *Proceedings Fourth International Conference on Computer Vision*, pages 173–182, Los Alamitos, California, 1993. IEEE Computer Society Press.
9. K. Chen and X.-C. Tai. A nonlinear multigrid method for curvature equations related to total variation minimization. Report 05-26, UCLA CAM, 2005.
10. P. M. de Zeeuw. Matrix–dependent prolongations and restrictions in a blackbox multigrid solver. *J. Comput. Appl. Math.*, 33:1–27, 1990.
11. P. M. de Zeeuw. Chapter 14: Multigrid and advection. In C. B. Vreugdenhil and B. Koren, editors, *Numerical Methods for Advection-Diffusion Problems*,

volume 45 of *Notes on Numerical Fluid Mechanics*, pages 335–351. Vieweg, Braunschweig, 1993.
12. P. M. de Zeeuw. A toolbox for the lifting scheme on quincunx grids (lisq). CWI Report PNA-R0224, Centrum voor Wiskunde en Informatica, Amsterdam, 2002. http://www.cwi.nl/ftp/CWIreports/PNA/PNA-R0224.pdf.
13. P. M. de Zeeuw. A multigrid approach to image processing. In R. Kimmel, N. Sochen, and J. Weickert, editors, *Scale Space and PDE Methods in Computer Vision*, volume 3459 of *Lecture Notes in Computer Science*, pages 396–407. Springer-Verlag, Berlin Heidelberg, 2005.
14. W. Hackbusch. *Multi-Grid Methods and Applications*, volume 4 of *Computational Mathematics*. Springer–Verlag, Berlin, 1985.
15. H. J. A. M. Heijmans and J. Goutsias. Multiresolution signal decomposition schemes. part ii: Morphological wavelets. *IEEE Trans. Image Process.*, 9(11):1897–1913, 2000.
16. R. Kimmel and I. Yavneh. An algebraic multigrid approach for image analysis. *SIAM J. Sci. Comput.*, 24(4):1218–1231, 2003.
17. S. Mallat. A theory for multiresolution signal decomposition: the wavelet representation. *IEEE Pattern Anal. Mach. Intell.*, 11(7):674–693, 1989.
18. P. Perona and J. Malik. Scale space and edge detection using anisotropic diffusion. *IEEE Pattern Anal. Mach. Intell.*, 12(7):629–639, 1990.
19. P. Perona, T. Shiota, and J. Malik. Anisotropic diffusion. In Bart M. ter Haar Romeny, editor, *Geometry-Driven Diffusion in Computer Vision*, volume 1 of *Computational Imaging and Vision Series*, pages 73–92. Kluwer Academic Publishers, Dordrecht, The Netherlands, 1994.
20. Y. Shapira. *Matrix-Based Multigrid: Theory and Applications.* Kluwer Academic Publishers, Boston, 2003.
21. E. P. Simoncelli and W. T. Freeman. The steerable pyramid: a flexible architecture for multi-scale derivative computation. In *Proceedings of the IEEE International Conference on Image Processing*, pages 444—447. IEEE Signal Processing Society, 1995.
22. W. Sweldens. The lifting scheme: A construction of second generation wavelets. *SIAM J. Math. Anal.*, 29(2):511–546, 1997.
23. D. Terzopoulos. Image analysis using multigrid relaxation methods. *IEEE Trans. Pattern Anal. Mach. Intell.*, 8:129–139, 1986.
24. U. Trottenberg, C. W. Oosterlee, and A. Schüller. *Multigrid.* Academic Press, London, 2001.
25. J. Weickert. *Anisotropic Diffusion in Image Processing.* Teubner-Verlag, Stuttgart, 1998.
26. P. Wesseling. *An Introduction to Multigrid Methods.* John Wiley & Sons Ltd., Chichester, 1991.